Video Article

Controlled Microfluidic Environment for Dynamic Investigation of Red Blood Cell Aggregation

Rym Mehri[1], Catherine Mavriplis[1], Marianne Fenech[1]

[1]Department of Mechanical Engineering, University of Ottawa

Correspondence to: Catherine Mavriplis at catherine.mavriplis@uottawa.ca

URL: http://www.jove.com/video/52719
DOI: doi:10.3791/52719

Keywords: Bioengineering, Issue 100, Red blood cells, aggregation, microcirculation, microfluidics, micro particle image velocimetry, blood rheology

Date Published: 6/4/2015

Citation: Mehri, R., Mavriplis, C., Fenech, M. Controlled Microfluidic Environment for Dynamic Investigation of Red Blood Cell Aggregation. *J. Vis. Exp.* (100), e52719, doi:10.3791/52719 (2015).

Abstract

Blood, as a non-Newtonian biofluid, represents the focus of numerous studies in the hemorheology field. Blood constituents include red blood cells, white blood cells and platelets that are suspended in blood plasma. Due to the abundance of the RBCs (40% to 45% of the blood volume), their behavior dictates the rheological behavior of blood especially in the microcirculation. At very low shear rates, RBCs are seen to assemble and form entities called aggregates, which causes the non-Newtonian behavior of blood. It is important to understand the conditions of the aggregates formation to comprehend the blood rheology in microcirculation. The protocol described here details the experimental procedure to determine quantitatively the RBC aggregates in microcirculation under constant shear rate, based on image processing. For this purpose, RBC-suspensions are tested and analyzed in 120 x 60 µm poly-dimethyl-siloxane (PDMS) microchannels. The RBC-suspensions are entrained using a second fluid in order to obtain a linear velocity profile within the blood layer and thus achieve a wide range of constant shear rates. The shear rate is determined using a micro Particle Image Velocimetry (µPIV) system, while RBC aggregates are visualized using a high speed camera. The videos captured of the RBC aggregates are analyzed using image processing techniques in order to determine the aggregate sizes based on the images intensities.

Video Link

The video component of this article can be found at http://www.jove.com/video/52719/

Introduction

Red Blood Cells (RBCs) play a crucial role in determining the rheological behavior of blood. They are almost singularly responsible for the particular properties of blood *in vitro* and *in vivo*. Under physiological conditions, RBCs occupy 40% to 45% of the blood volume. In microcirculation, RBCs only occupy up to 20% of the blood volume due to smaller vessel diameters and the plasma skimming effect[1]. This phenomenon of plasma reduction in microcirculation is known as the Fåhræus effect. At low shear rates, RBCs are able to bridge together and form one dimensional or three dimensional structures called “rouleaux” or aggregates, hence contributing to the non-Newtonian behavior of blood. However, the mechanism of RBC aggregation is not completely understood. Two theories exist to model the aggregation of RBCs: the bridging of cells theory due to the cross-linking of the macromolecules[2] and the force attraction theory caused by depletion of the molecules due to the osmotic gradient[3].

Typically, for human blood, aggregates form at very low shear rates[4] ranging from 1 to 10 sec^{-1}. Above this range, RBCs tend to disaggregate and flow separately within the vessel.

Understanding the conditions of the aggregates formation is of a great importance to the hemorheology field in terms of defining blood’s rheological behavior. These aggregates are often seen at the macrocirculation level (>300 µm diameter)[5]. At this scale, blood is considered as a Newtonian fluid and a homogenous mixture. However, these aggregates are rarely seen in the capillary level (4-10 µm in diameter) and are usually an indication of pathological conditions such as diabetes[6] and obesity. Other pathological conditions that could change RBC aggregation include inflammatory or infectious conditions, cardiovascular diseases such as hypertension or atherosclerosis, genetic disorders and chronic diseases[7]. Therefore, understanding the RBC aggregation mechanism and analyzing these entities (by defining a relationship between the size of these aggregates and the flow conditions) could lead to the understanding of the microrheological behavior of blood and hence relate it to clinical applications.

RBC aggregates can be altered by several factors such as the hematocrit (volume of RBCs in blood), the shear rate, the vessel diameter, the RBC membrane stiffness and the suspending medium composition[8-10]. Therefore, controlled conditions are required in order to effectively analyze the RBC aggregates. Several methods are able to analyze aggregate formation by providing static aggregation measurements (aggregation index) that offers relevant information about blood behavior. These methods include, inter alia, the erythrocyte sedimentation rate method[11], the light transmission method[12], the light reflection method[13] and the low shear viscosity method[14].

Few studies have attempted to study RBC aggregation and determine the degree of aggregation in controlled flow conditions[15-17]. However, these studies indirectly investigate RBC aggregate sizes by determining the ratio of the occupied space in a shearing system measured based

on microscopic blood images providing information on the degree of aggregation as well as the local viscosity. Chen *et al.*[18] presented a direct measurement technique for RBC aggregate sizes and provided RBC aggregate size distribution for different shear stresses by varying the flowrate of the suspensions while monitoring the pressure drop across a flow chamber. The shear stresses are calculated based on the monitored pressure using Stokes equation[18].

We therefore present a new procedure to directly quantify RBC aggregates in a controlled microfluidic environment, dynamically, under specific, constant and measurable shear rates. The blood flow in the shear system is directly observed (perpendicularly to the flow direction), providing a different angle on flow investigation compared to previous studies[15,18] and a visualization of the full domain of interest. RBC-suspensions are entrained, in a double Y-microchannel (as illustrated in **Figure 1**), with a Phosphate Buffered Saline (PBS) solution hence creating a shear flow in the blood layer. Within this blood layer a constant shear rate can be obtained. The RBC-suspensions are tested at different hematocrit (H) levels (5%, 10% and 15%) and under different shear rates (2-11 sec^{-1}). The blood velocity and shear rate are determined using a micro Particle Image Velocimetry (μPIV) system while the flow is visualized using a high speed camera. The results obtained are then processed with a MATLAB code based on the image intensities in order to detect the RBCs and determine aggregate sizes.

Protocol

Blood is collected from healthy individuals with the approval of the ethics committee of the University of Ottawa (H11-13-06).

1. Microchannel Fabrication

The microchannels are fabricated based on the standard photolithography methods[19].

1. Design the microchannel geometry using a Computer Aided Design (CAD) software and print the configuration on a transparency photo-mask. These masks are crucial since they dictate the light path during the fabrication process. In this case, the microchannel dimensions are 120 μm in thickness, 60 μm in depth and 7 mm in length.
2. In a cleanroom, spin coat an epoxy based negative photo-resist on a silicon wafer at 2,000 rpm for 30 sec to obtain the desired microchannel depth (60 μm).
3. Expose the wafer and the photo-mask under a UV lamp at 650 mJ/cm^2 for 70 sec. Ensure to expose only the transparent areas of the photo-mask to the UV-light. The exposure of the transparent areas allows for polymerization of the chains resulting in a hardening of the photo-resist. Immerse the silicon piece into a developer to remove excess of photo-resist.
4. Once the mold is fabricated, mix a silicon based elastomer and a curing agent at a ratio of 10:1 to create a solution of poly-dimethyl-siloxane (PDMS). Put the PDMS solution in a vacuum chamber to degas. Pour it into the mold and heat it at 60 °C for 90 min to create microchannels. Then bond the individual channels to a glass slide using oxygen plasma bonding for 90 sec.
   NOTE: the PDMS degas process is performed in order to eliminate the air bubbles engendered by the mixing process.
5. Ensure that the microchannel dimensions allow for successful testing. In this protocol, the microchannels have a rectangular cross-section of 120 x 60 μm. In comparison, an average RBC has a diameter of 8 μm and a thickness of 2 μm. Therefore, the microchannel width is sufficient to observe proper aggregation and accurately determine the velocity profiles.

2. Blood Preparation

1. Collect blood from healthy volunteer donors, after approval of an ethics committee. Treat the blood with ethylenediaminetetraacetic acid (EDTA) present in the collection tubes (7.2 mg EDTA in 4 ml of blood).
   NOTE: The EDTA is used to avoid blood clotting.
2. Centrifuge the blood samples three times for 10 min at 1,400 x g (3,000 rpm) in order to separate the blood constituents. As a result of the centrifugation, observe three distinct layers.
   NOTE: The three layers are the RBC layer (located at the bottom of the tube), the buffy coat (consisting of white blood cells and platelets located on top of the RBC layer) and the plasma layer (located on top of all the other constituents).
   1. After the first centrifugation, collect blood plasma using a blood pipette. Avoid any contact with the buffy coat.
   2. Collect and dispose of the buffy coat in a container with bleach diluted at 10%.
   3. Add 3 ml of PBS pH 7.4 to each of the tubes with the remaining RBC layer and ensure the proper balance of the centrifuge. Gently mix the tubes and centrifuge once again at 1,400 x g (3,000 rpm) for 10 min.
      NOTE: Ensure that the PBS solution does not contain any Magnesium or Calcium since they could alter the cell adhesion.
   4. Dispose of the PBS in the tubes after the second centrifugation and remove the remaining buffy coat if present. Repeat steps 2.2.3 and 2.2.4 for the third centrifugation to yield clean RBCs.
3. Mix the required amount (0.05, 0.1 and 0.15 ml) of the clean RBCs with plasma (0.95, 0.9 and 0.85 ml) in a 1 ml tube in order to obtain RBC-suspensions with the corresponding (5%, 10% and 15%) hematocrit. Check hematocrits with a microcentrifuge.

3. Fluids Preparation

Introduce two fluids in the double Y-microchannel: RBC-suspensions and PBS.

1. Add 60 μl of the fluorescent tracer particles solution (1% solid, $d_{particle}$ = 0.86 μm, λ_{abs} = 542 nm and $\lambda_{emission}$ = 612 nm) into the 1 ml RBC-suspension tubes.
   NOTE: The fluorescent tracer particles (internally dyed polystyrene particles) are used to measure the velocity of the flow within the microchannel. These particles fluoresce when exposed to the corresponding wavelength of the laser beam (λ = 542 nm).
2. Prepare a PBS pH 7.4 solution and add 60 μl of the same fluorescent tracer particles solution in 1 ml of the PBS solution.

4. Aggregates Size Measurements

1. To insert the fluids (RBC-suspensions and PBS) in the microchannel, use two glass syringes of 25 µl and 100 µl. This will help to reduce the compliance of the system. Connect the microchannel to the syringes via tubing and connectors fitting the entry holes. Fill the glass syringes using the pressure difference existing between the fluid container and the syringe. Ensure no bubbles are present in the system. As an alternative method, use a pressure controlled system to drive both fluids in the microchannel.
2. Place the microchannel on an inverted microscope stage connected to a high speed camera and a µPIV system. Program the syringe pump to the desired flow rates (*e.g.,* Q = 2 µl/hr for blood engendering a flowrate of Q = 8 µl/hr for PBS).
   NOTE: Only one syringe pump is used. Using two different glass syringes, with two different internal diameters, it is possible to vary to the flowrate entering each branch of the Y-microchannel.
3. Insert both fluids in the double Y-microchannel each from a different entry branch and at different flowrates as shown in **Figure 1**. In order to test different shear rates, change the pump flowrate. This maintains the same appropriate ratio (4 in this case) between the two branches[20] (**Figures 2** and **3**). Wait for the flow to reach steady state before acquiring the measurements: visually inspect the high speed camera images for a smooth flow.
   NOTE: The ratio is crucial in obtaining a linear velocity profile within the blood layer.
4. Visualize the RBCs using the high speed camera. Connect the camera to a computer to control, record and save the images of the fluid flow. Once the two fluid flows reach steady state, start recording.
   1. Acquire several images for better processing results. Determine an optimal camera exposure time for a clear image of the aggregates.
      NOTE: The camera exposure time for this case was 0.5 msec. The choice of time interval between each frame is based on the camera frame rate and the flow rate in the microchannel. The time between each frame processed in this procedure was 60 msec. Therefore a camera capable of recording 18 frames per seconds is sufficient.
      NOTE: Avoid blood settling in the tube and syringe, which could lead to erroneous measurements.

5. Using image processing techniques (a MATLAB program in this case) to ameliorate the image quality, detect the aggregates in each of the images based on pixel intensities (illustrated in **Figure 4**) as follows:
   1. Enhance the images contrast using the histogram equalizer method to obtain a better image quality for each frame.
   2. Convert the greyscale images into binary images. For this purpose, set a threshold value, ranging from 0 to 1, that dictates the conversion of each pixel. Any pixel in the image below the threshold value will be detected as a black pixel, while the pixels with values larger than the threshold will be detected as white pixels.
   3. Fill the holes (if present and necessary) corresponding to the gaps within one aggregate for better results.
   4. Detect the cells by determining neighboring white pixels in the binary image so that adjacent cells are associated as aggregates.
   5. Label the different aggregates detected and convert the binary image into a red-green-blue (RGB) image for better visualization. Combine the original frames with each of the corresponding processed images to verify the efficiency of the image processing technique and ensure that all the cells are taken into consideration, as shown in **Figure 5**. Perform steps 4.5.1, 4.5.2, 4.5.3, 4.5.4 and 4.5.5 for all the frames captured.
   6. Calculate the area of each aggregate detected in the frame based on the number of pixels detected. Based on the lens magnification used, calculate the conversion factor, using a calibration reticule, and convert the results to μm^2. Average the aggregate sizes detected in each frame and then average the results for all frames to obtain the average aggregate size for each recording of RBC-suspensions.
   7. Calculate the area of one RBC to determine a representative estimated number of RBCs within each detected aggregate. Using these results, calculate the distribution of the percentage of RBCs within each aggregate as a function of the aggregate sizes (represented by the estimated number of cells in each aggregate), as shown in **Figure 6**.
      NOTE: To measure the RBC aggregates, ImageJ software could be used (instead of MATLAB) to perform the same tasks on each frame.

5. Fluid Velocity and Shear Rate Measurements

Determine the fluid velocity and hence the shear rate using a µPIV system.

1. Once the data is acquired using the high speed camera, switch to the double pulsed camera used for the µPIV system. Use an imaging software for image acquisition of the flow and the image processing for velocity field determination.
2. Take all the precautions necessary, depending on the class of the laser, before turning on the laser. Then turn on the system, the camera and the laser.
3. Calibrate the camera based on the lens magnification used. For this purpose, use a microscale of 10 µm precision under the microscope and set the size of 1 pixel in the image.
4. Start the laser and visualize the particles in both fluids. Find the middle plane of the microchannel by focusing on the fastest particles in the flow (*i.e.,* the fastest particles should be the brightest).
5. Set the dt (time interval between two consecutive frames) to ensure the proper displacement of the particle. The fastest particles should move about 5 to 10 pixels between both images.
6. Start recording the flow. Set the software to acquire 100 pairs of images, 5 msec apart. Perform steps 5.4, 5.5 and 5.6 for all the different RBC-suspensions and for different shear rates.
   NOTE: More details of the methodology are given in the study of Pitts and Fenech[21].
7. Process the recordings acquired using the cross-correlation method with the imaging software.
   NOTE: This consists of discretizing the pair of images into small windows of predetermined size (based on the fluid flow and the time interval chosen by the user) called correlation windows and following the displacement of the particles in each window.
   1. First, determine if the images acquired require pre-processing (including background subtraction, "base-clipping"[22] or image overlapping[23,24]) for better data processing.
   2. Then choose the correlation window size and shape, as well of the percentage of images overlapping. A detailed study was performed by Pitts *et al.*[25] to determine the optimal parameters and image pre-processing techniques for blood flow in different channel

configurations. Express the results as an average velocity field calculated from the 100 image pairs and the Root Mean Square (RMS) error in velocity.

8. Extract a velocity profile at the channel outlet, from the processed data as shown in **Figure 7**. For a better profile, average the velocity field in space.
   NOTE: The bars composing the velocity profile correspond to the correlation window size chosen relative to the channel width. The RMS error in velocity is also shown in **Figure 7**, representing the error in the experimental velocity estimation.
9. Turn off the laser once all the measurements and processing are performed,. Shut down all the components of the system: software, cameras, moving stage, computers and laser.
10. To calculate the shear rate, first detect and estimate the blood thickness in the microchannel based on the high speed camera recording. For this purpose, average all the frames in the specific recording to obtain a background image of the video. Delimit the blood layer (as shown in **Figure 8** for the RBC-suspensions flowing at 10 µl/hr when suspended at 5%, 10% and 15% hematocrit). Obtain the velocity value for the corresponding blood layer thickness and calculate the shear rate by dividing the velocity value by the blood layer thickness.

Representative Results

An example of the two-fluid flow in the double Y-microchannel is shown in **Figure 2** for human RBCs suspended at 5%, 10% and 15% hematocrit and flowing at 10 µl/hr. **Figure 3** shows the difference in aggregate sizes when the flow in the channel is reduced from 10 µl/hr to 5 µl/hr for a hematocrit of 10%. This gives a qualitative notion of the sizes of the aggregates when varying the hematocrit and shear rate. **Figure 5** follows the displacement of four human RBC aggregates, for three consecutive frames, providing a qualitative measure of the camera frame rate required and qualitative notion of the aggregates distribution within each frame. In **Figure 5**, the small aggregates (with 8 or less estimated RBCs) are shown in blue, while medium aggregates (ranging from 9 to 30 estimated RBCs) and large aggregates (greater than 30 estimated RBCs) are shown in green and red respectively.

The velocity profiles of the different RBC-suspensions in the channel are displayed in **Figure 7**, where the red, blue and green curves represent the velocity profiles of the RBCs suspended at 5%, 10% and 15% hematocrit respectively. The RMS errors of the velocity, also displayed in **Figure 7** for each RBC-suspension, are relatively small compared to the velocity values, indicating the precision of the velocity measurements, and hence shear rates. The interface locations are denoted as 'E' and shown as the solid lines in the same figure.

The corresponding shear rates for the different RBC-suspensions (based on the velocity profiles and the blood layer thickness) are shown in **Table 1**. The average aggregate sizes determined for each of the RBC-suspensions, based on the image processing method to detect the area of the RBC aggregates, are shown in **Figure 9**, as a function of the corresponding shear rate. An example of the distribution of the percentage of RBCs within each aggregate is shown in **Figure 6**. The aggregate sizes are represented as an estimated number of RBC in the aggregates.

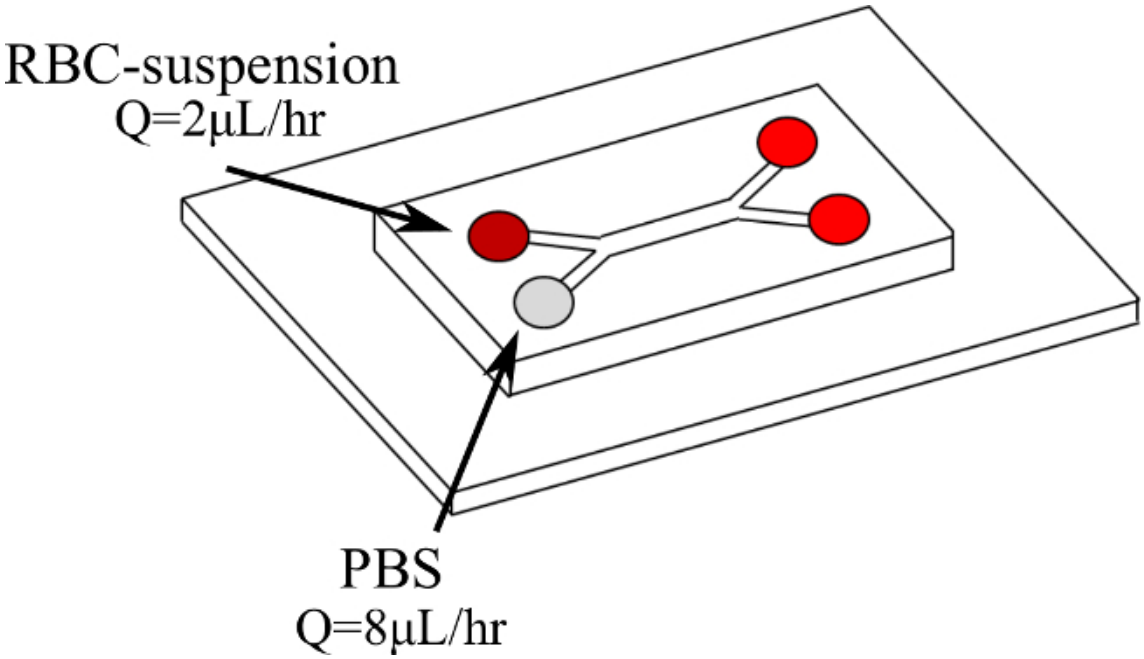

Figure 1. Double Y-microchannel configuration and entry fluids. Blood enters the first branch at Q = 2 µl/hr while PBS enters the second branch at Q = 8 µl/hr. Please click here to view a larger version of this figure.

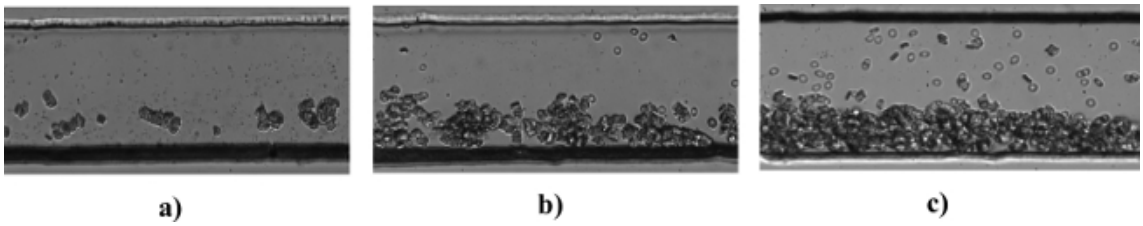

Figure 2. Human RBC-suspension at different hematocrit. The figure represents captured frames of the human RBC-suspensions flowing at Q = 10 µl/hr at (**A**) 5% (**B**) 10% and (**C**) 15% hematocrit. Please click here to view a larger version of this figure.

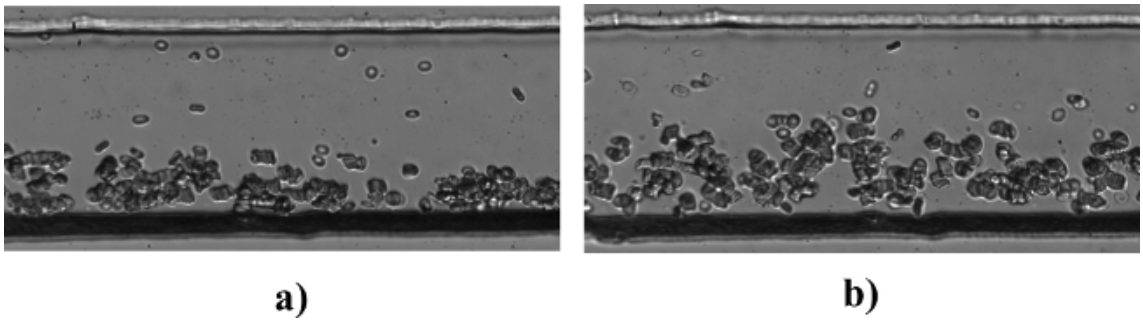

Figure 3. Human RBC-suspension at different flowrates. The figure represents captured frames of the human RBCs suspended at 10% hematocrit H flowing (**A**) Q = 10 µl/hr and (**B**) Q = 5 µl/hr. Please click here to view a larger version of this figure.

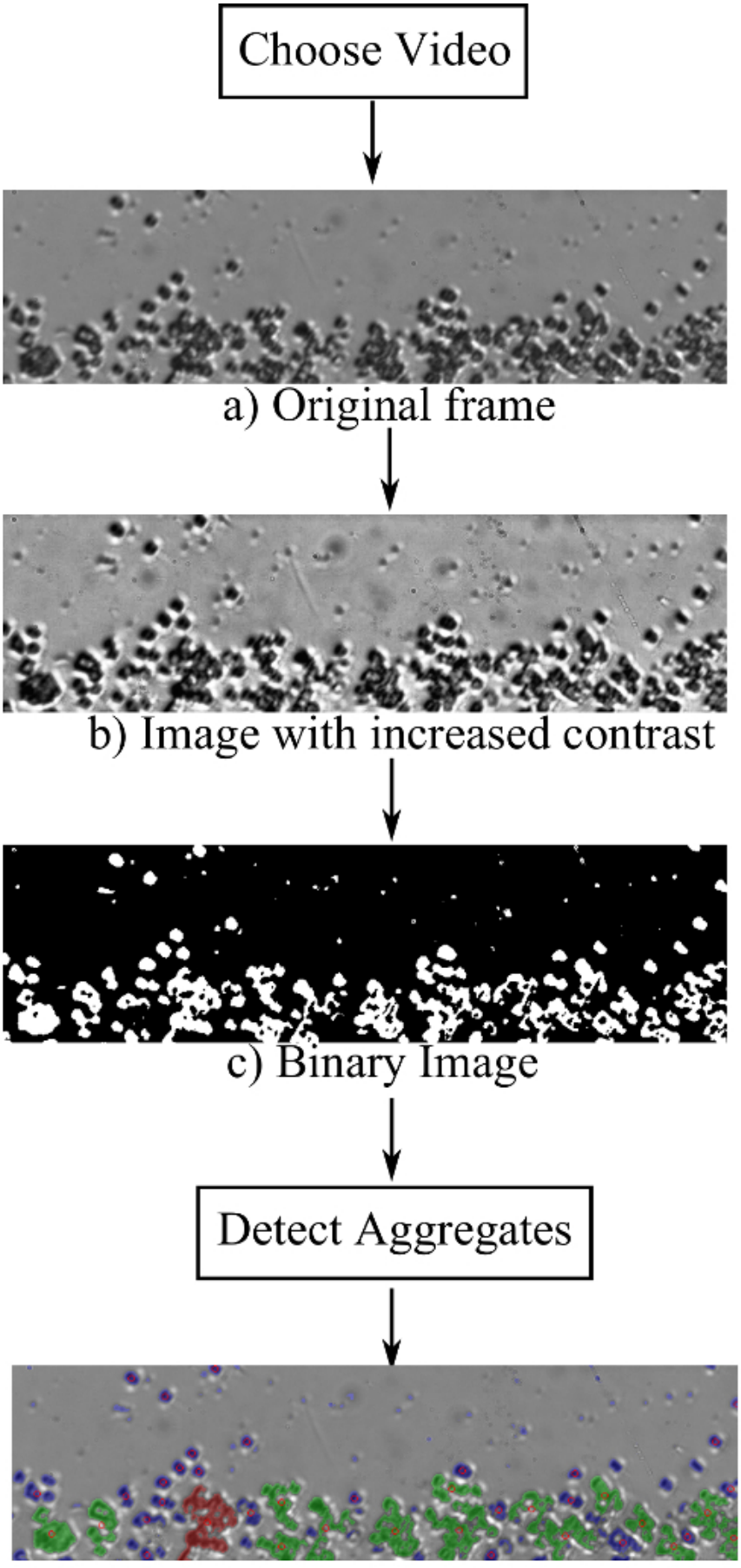
Choose Video
a) Original frame
b) Image with increased contrast
c) Binary Image
Detect Aggregates
d) Original Image combined to labeled RGB Image

Figure 4. Flow chart of the image processing program used for aggregate detection. The steps shown describe the basic methodology used. The quality of the image is enhanced to be converted to a binary image. The aggregates are detected and labeled based on their respective sizes. Please click here to view a larger version of this figure.

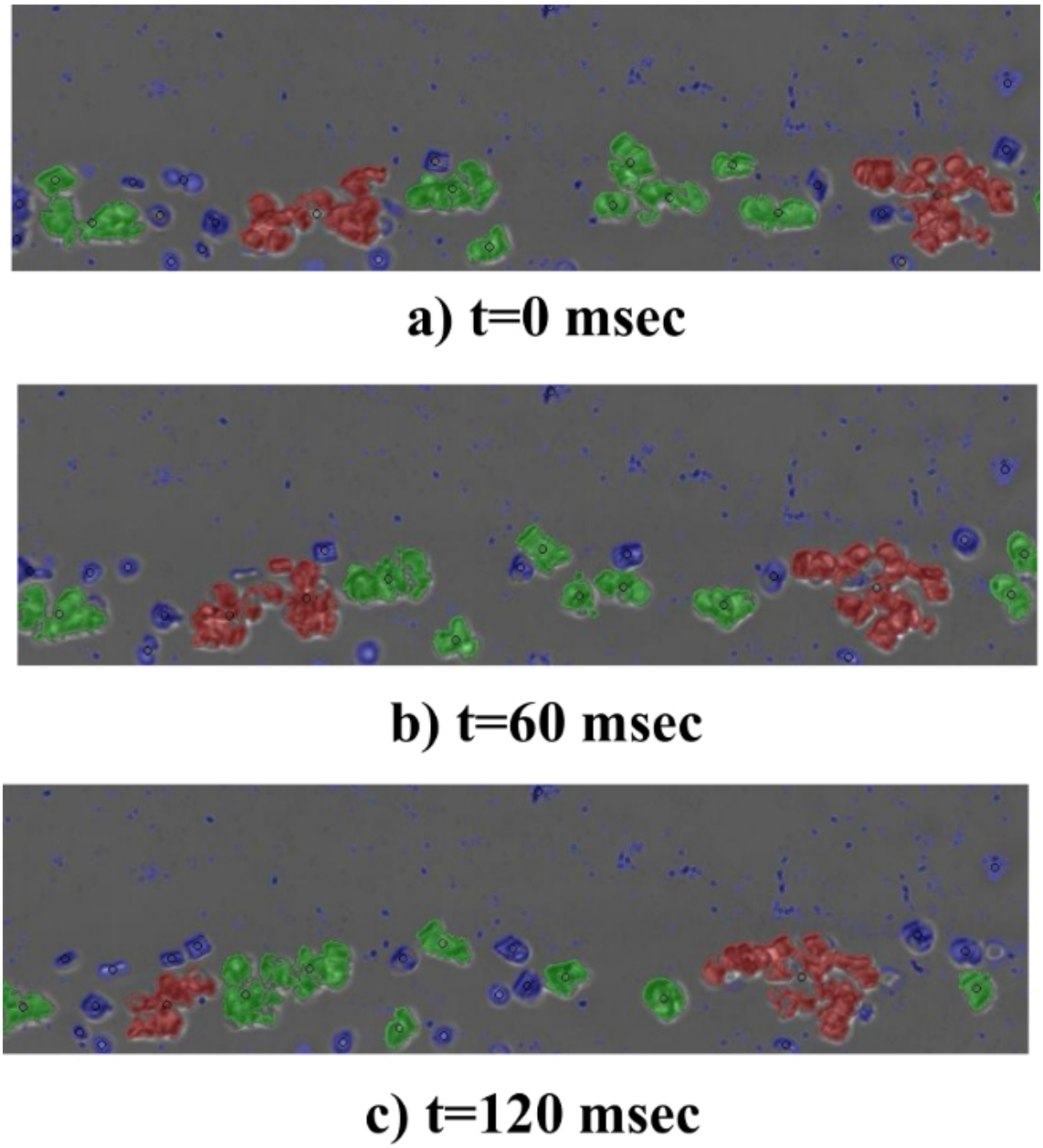

Figure 5. RGB coloring and net motion of the several human RBC aggregates for three consecutive frames. The figure shows the net motion of four aggregates detected in three consecutive frames at (**A**) t = 0 msec, (**B**) t = 60 msec and (**C**) t = 120 msec. The large aggregates (> 30 estimated RBCs), medium aggregates (9-30 estimated RBCs) and small aggregates (<8 estimated RBCs) are shown in red, green and blue respectively. Each of the aggregates detected are marked with a black circle. Please click here to view a larger version of this figure.

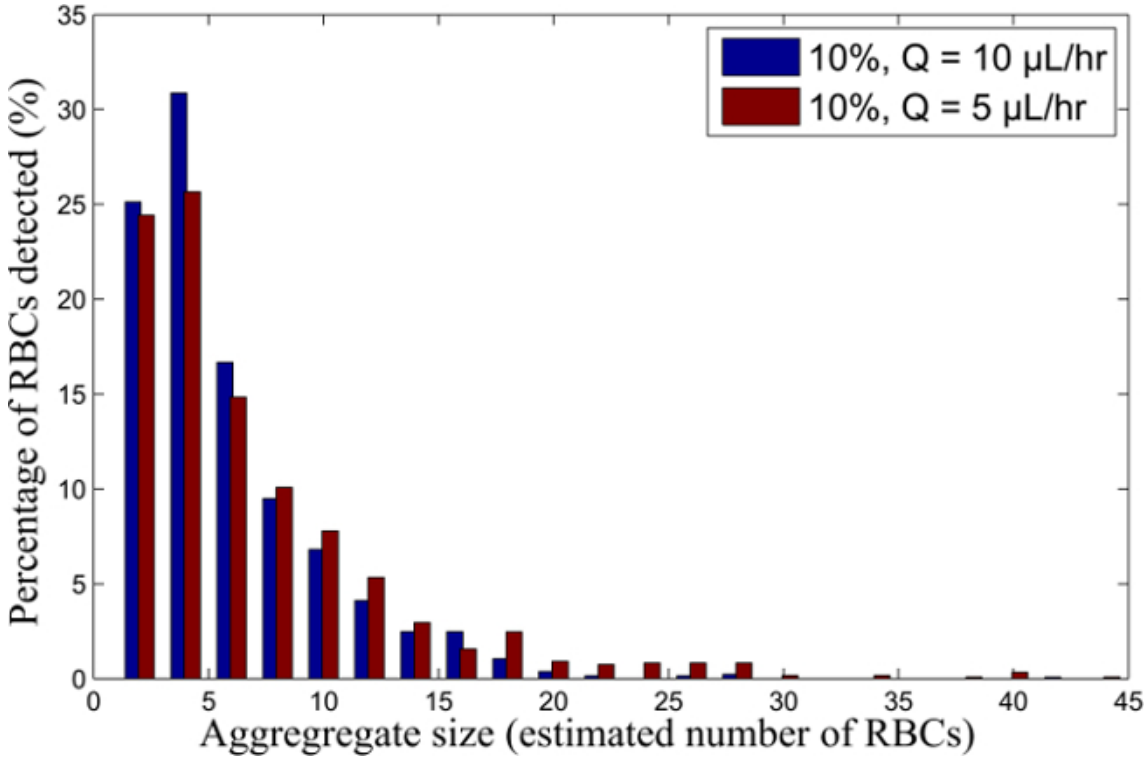

Figure 6. RBC aggregate size distribution for 10%H RBC-suspension for different flow rates. Aggregate size distribution for blood samples suspended at 10% H, flowing at Q = 10 and 5 µl/hr. Please click here to view a larger version of this figure.

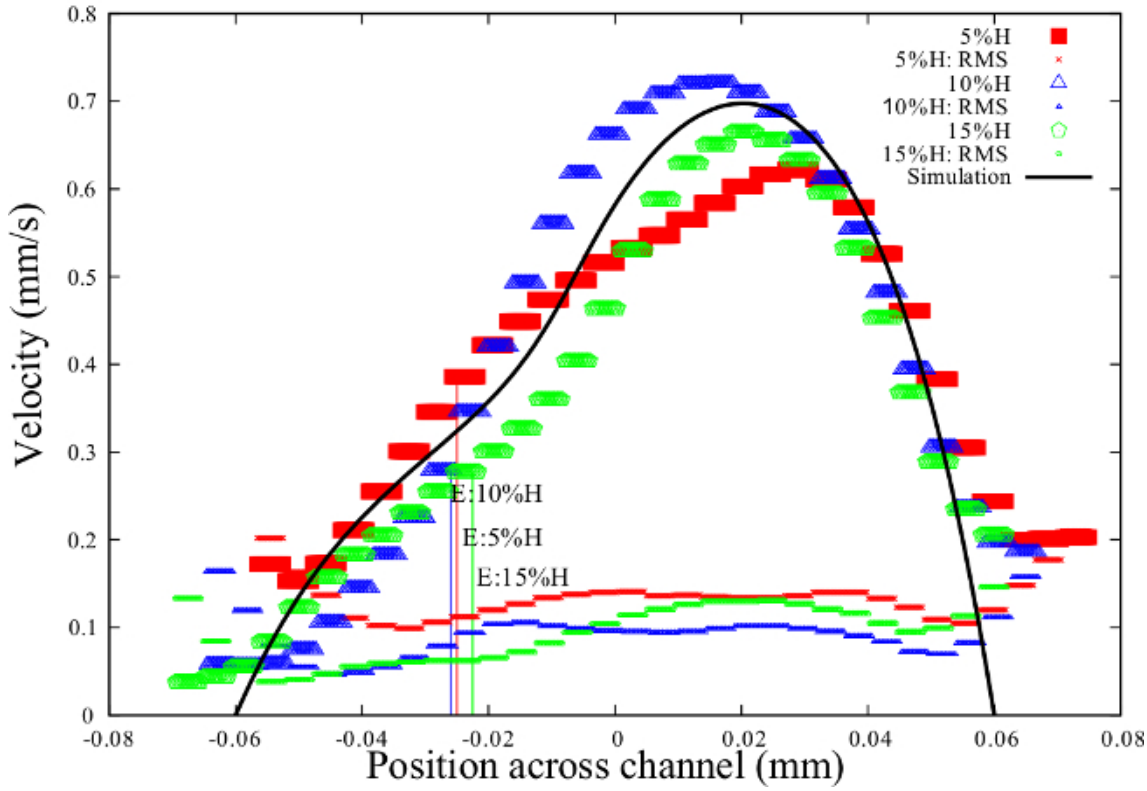

Figure 7. Velocity profile comparison for different hematocrit. The velocity profiles are shown for RBCs in plasma suspended at 5% H (Red), 10% H (blue), 15%H (green) and simulation[20] (solid line) for the 120 x 60 µm double Y-microchannel with a Q = 10 µl/hr. The interface location is denoted by E for the experiments. The corresponding RMS errors of the different velocity profiles are displayed. Please click here to view a larger version of this figure.

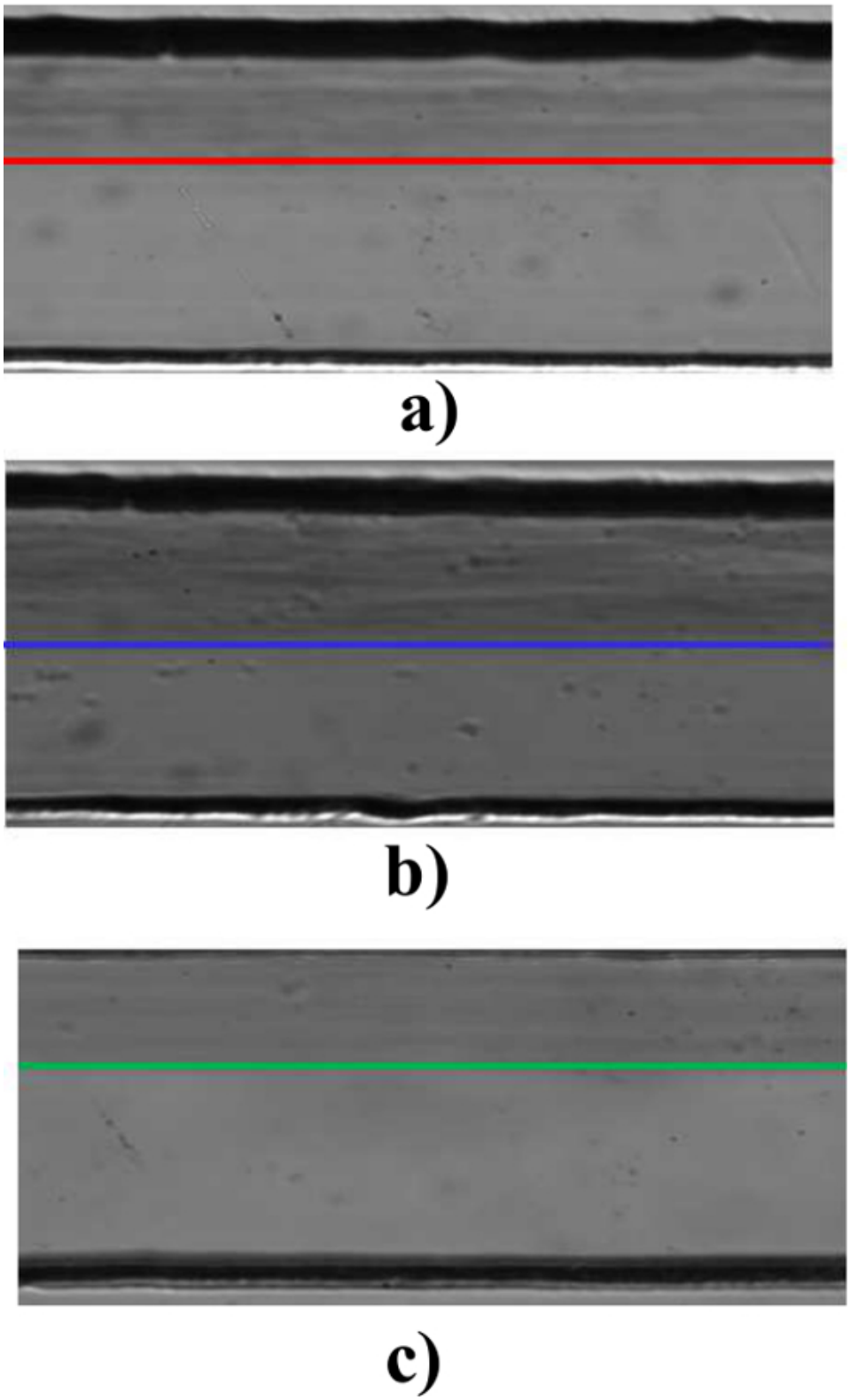

Figure 8. Image background for the different RBC-suspensions and delimitation of the blood layer thickness. The figure shows the delimitation of the blood layer thickness of the RBC-suspensions flowing at 10 µl/hr suspended at (**A**) 5%, (**B**) 10% and (**C**) 15% H. Please click here to view a larger version of this figure.

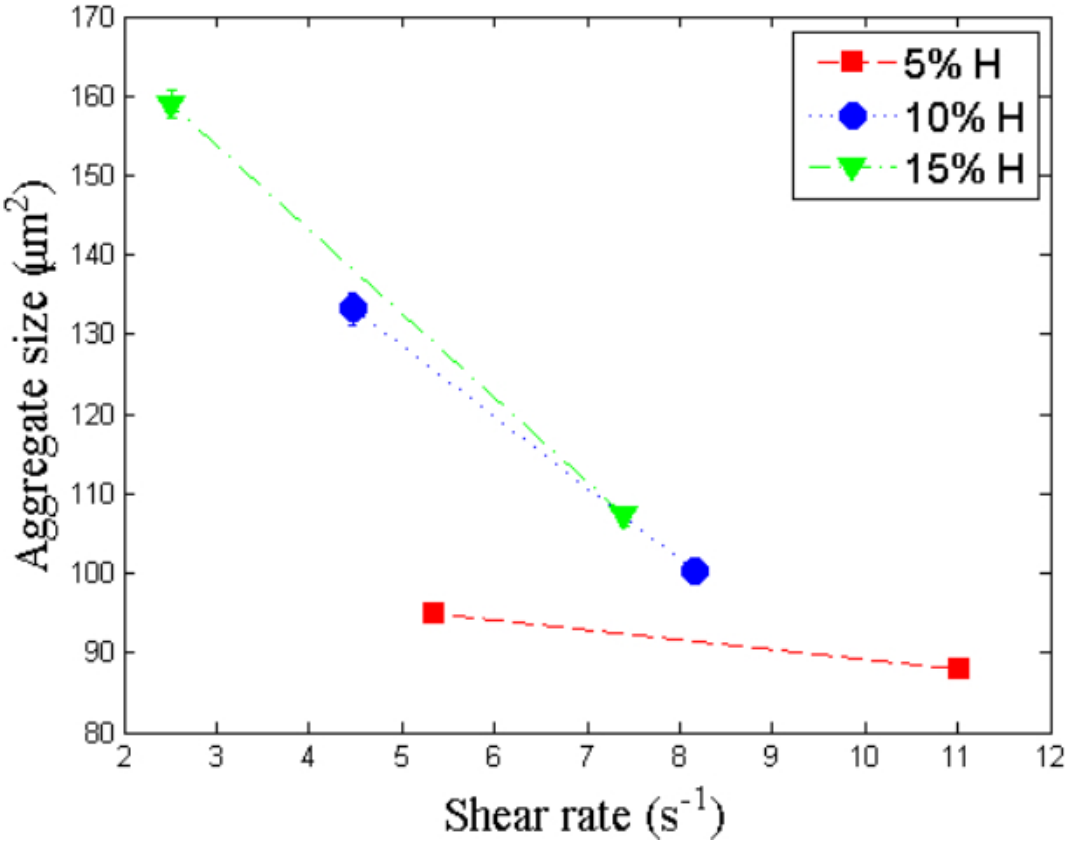

Figure 9. **Average aggregate sizes as a function of the corresponding shear rates**. The results are obtained for the different RBC-suspensions flowing at Q = 10 µl/hr at 5% (**A**), 10% (**B**) and 15% H (**C**). Please click here to view a larger version of this figure.

Hematocrit	Flow rate (µl/hr)	Shear rate (sec^{-1})
5%	10	11.02
5%	5	5.36
10%	10	8.17
10%	5	4.47
15%	10	7.41
15%	5	2.51

Table 1. Shear rate values for different blood flow cases. The shear rate values are obtained using the µPIV data and image processing results for different RBC-suspensions with 5%, 10% and 15% H, flowing at Q = 10 µl/hr and Q = 5 µl/hr.

Discussion

Using the present methodology, it is possible to analyze qualitatively and quantitatively the RBC aggregates under different flow conditions and hematocrits. For successful testing and aggregate detection, it is crucial to determine the appropriate velocity ratio between the two fluids at the microchannel entry. This ratio is very important to obtain an optimal blood layer thickness where the velocity profile is quasi-linear[20].

Another key factor for successful testing is a good image quality. In fact, since the method is based on image processing, it is very important to have a contrast between the image background (the fluid inside the channel) and the particles to be detected. Here, as shown in **Figures 2** and **3**, the particles appear to be darker than the background, which helps in the aggregate detection. The most important parameter to consider for the image processing technique is the threshold value. Therefore, based on the contrast obtained it is crucial to choose the optimal threshold value where all the aggregates will be taken into consideration, as shown in **Figure 5**. The present image segmentation, used for this study, is widely used for cell detection and counting[26-28]. If the quality of the image is not as desired and a global threshold value is not appropriate, one can use a different algorithm to determine the optimal threshold value such as Otsu's method[29] or an adaptive thresholding method (discretizing the image and obtaining a local threshold for each discretized window).

Another factor to take into account is the scale factor for a proper conversion from pixels to µm.

Using the proper conversion factor, one can determine the diameter and thickness of one RBC that will serve to determine the aggregate size distribution (based on the estimated number of RBCs in each aggregate). Depending on the orientation of the aggregates, properly calculate the

area on one RBC (frontal or side view). As mentioned in section 4 (step 4.4.1), it is important to determine the proper camera exposure time and the frame rate to ensure that the dynamic properties of the aggregates are captured between each consecutive frame. This value is based on the flow rate used when acquiring the measurements. Several other factors need to be taken into consideration when acquiring results using the μPIV system and are discussed clearly in the study of Pitts and Fenech[21].

The methodology was tested successfully on several RBC-suspensions flowing at different hematocrit. However, due to the limitation of the image processing technique and the lack of contrast between the image background and the aggregates, it is difficult to detect the RBC aggregates for higher hematocrits (from 20% to 45%). Indeed as mentioned previously, the image quality is crucial for this methodology.

Using this protocol, the RBC aggregate sizes can be measured in a controlled microfluidic device and hence it is possible to obtain information on RBC aggregation dynamically in microcirculation and obtain the RBC aggregate sizes for a range of physiological shear rates. It is also possible to complement numerical and experimental studies of blood rheology and relate the aggregate sizes and behavior to clinical and pathological studies.

Disclosures

The authors have nothing to disclose.

Acknowledgements

This work was supported by the Natural Sciences and Engineering Research Council of Canada. Microfabrication was performed with the support of the McGill Nanotools Microfab facility at McGill University and the Department of Electronics at Carleton University.

References

1. Perkkio, J., Keskinen, R. Hematocrit reduction in bifurcations due to plasma skimming. *Bull. Math. Biol.* **45**, (1), 41-50 (1983).
2. Chien, S., Jan, K. Ultrastructural basis of the mechanism of rouleaux formation. *Microvasc. Res.* **5**, (2), 155-166 (1973).
3. Neu, B., Meiselman, H. J. Depletion-mediated red blood cell aggregation in polymer solutions. *Biophys. J.* **83**, (5), 2482-2490 (2002).
4. Schmid-Schönbein, H., Gaehtgens, P., Hirsch, H. On the shear rate dependence of red cell aggregation in vitro. *J. Clin. Invest.* **47**, (6), 1447-1454 (1968).
5. Pries, A. R., Secomb, W. Rheology of the microcirculation. *Clin. Hemorheol. Microcirc.* **29**, (3-4), 143-148 (2003).
6. Baskurt, O. K., Neu, B., Meiselman, H. J. *Red Blood Cell Aggregation.* Taylor and Francis Florida (2011).
7. Cho, Y. I., Mooney, M. P., Cho, D. J. Hemorheological disorders in diabetes mellitus. *J. Diabetes Sci. Technol.* **2**, (6), 1130-1138 (2008).
8. Baskurt, O. K., Hardeman, M. R., Rampling, M. W., Meiselman, H. J. *Handbook of Hemorheology and Hemodynamics.* IOS Press Netherlands (2007).
9. Lindqvist, T. The viscosity of the blood in narrow capillary tubes. *Am. J. Physiol.-Legacy Content.* **96**, 562-568 (1931).
10. Goldsmith, H. L., Cokelet, G. R., Gaehtgens, P. R. Fåhraeus: Evolution of his concepts in cardiovascular physiology. *Am. J. Physiol.* **257**, (3), H1005-H1015 (1989).
11. Fåhraeus, R. The suspension stability of the blood. *Physiol. Rev.* **9**, (2), 241-274 (1929).
12. Bauersachs, R. M., Wenby, R. B., Meiselman, H. J. Determination of specific red blood cell aggregation indices via an automated system. *Clin. Hemorheol.* **9**, (1), 1-25 (1989).
13. Hardeman, M. R., Dobbe, J. G., Ince, C. The laser-assisted optical rotational cell analyzer (lorca) as red blood cell aggregometer. *Clin. Hemorheol. Microcirc.* **25**, (1), 1-11 (2001).
14. Rampling, M. W. Red cell aggregation and yield stress. *Clinical Blood Rheology.* CRC Press Boca Raton, Florida (1988).
15. Dusting, J., Kaliviotis, E., Balabani, S., Yianneskis, M. Coupled human erythrocyte velocity field and aggregation measurements at physiological haematocrit levels. *J. Biomech.* **42**, (10), 1438-1443 (2009).
16. Kaliviotis, E., Dusting, J., Balabani, S. Spatial variation of blood viscosity: modelling using shear fields measured by a μPIV based technique. *Med. Eng. Phys.* **33**, (7), 824-831 (2011).
17. Sherwood, J. M., Kaliviotis, E., Dusting, J., Balabani, S. Spatial variation of blood viscosity and velocity distributions of aggregating and non-aggregating blood in a bifurcating microchannel. *Biomech. Model. Mechan.* **13**, (2), 259-273 (2014).
18. Chen, S., Barshtein, G., Gavish, B., Mahler, Y., Yedgar, S. Monitoring of red blood cell aggregability in a flow chamber by computerized image analysis. *Clin. Hemorhol. Microcirc.* **14**, (4), 497-508 (1994).
19. Xia, Y. N., Whitesides, G. M. Soft lithography. *Angewandte Chemie International Edition England.* 551-577 (1998).
20. Mehri, R., Mavriplis, C., Fenech, M. Design of a microfluidic system for red blood cell aggregation investigation. *J. Biomech. Eng.* **136**, (6), 064501-1-064501-5 (2014).
21. Pitts, K. L., Fenech, M. Micro-particle image velocimetry for velocity profile measurements of micro blood flows. *J. Vis. Exp.* (74), e50314 (2013).
22. Bitsch, L., Oleson, L. H., Westergaard, C. H., Bruus, H., Klank, H., Kutter, J. P. Micro particle-image velocimetry of bead suspensions and blood flows. *Exp. Fluids.* **39**, (3), 507-513 (2005).
23. Wereley, S. T., Gui, L., Meinhart, C. D. Advanced algorithms for microscale particle image velocimetry. *AIAA J.* **40**, (6), 1047-1105 (2002).
24. Nguyen, C. V., Fouras, A., Carberry, J. Improvement of measurement accuracy in micro PIV by image overlapping. *Exp. Fluids.* **49**, (3), 701-712 (2010).
25. Pitts, K. L., Mehri, R., Mavriplis, C., Fenech, M. Micro-particle image velocimetry measurement of blood flow: validation and analysis of data pre-processing and processing methods. *Meas. Sci. Technol.* **23**, (10), 105302 (2012).
26. Bhamare, M. G., Patil, D. S. Automatic blood cell analysis by using digital image processing: a preliminary study. *Int. J. Eng. Res. Tech.* **2**, (9), 3135-3141 (2013).

27. Maitra, M., Gupta, R. K., Mukherjee, M. Detection and counting of red blood cells in blood cell images using hough transform. *Int. J. Comput. Appl.* **53**, (16), 18-22 (2012).
28. Jambhekar, N. D. Red blood cells classification using image processing. *Sci. Res. Repot.* **1**, (3), 151-154 (2011).
29. Otsu, N. A threshold selection method from gray-level histograms. *IEEE Trans. Syst. Man. Cybern.* **9**, (1), 62-66 (1979).

